

PREPARATION AND CHARACTERIZATION OF SPION-CDs AS A MULTIFUNCTIONAL FLUORESCENCE/MAGNETIC RESONANCE NANOPARTICLE

Mahdi Asgari^a, Hasan Motaghi^b, Hossein Khanahmad^c, Masoud A. Mehrgardi^{b*}, Amin Farzadniya^d and Parvaneh Shokrani^{a*}

^a*Department of Medical Physics, School of Medicine, Isfahan University of Medical Sciences, Isfahan, Iran*

^b*Department of Chemistry, University of Isfahan, Isfahan, Iran*

^c*Department of Genetics and Molecular Biology, School of Medicine, Isfahan University of Medical Sciences, Isfahan, Iran*

^d*Department of Radiology, Askarieh hospital, Isfahan, Iran*

Abstract: A multifunctional nanoparticle, Super Paramagnetic Iron Oxide Nanoparticle-Carbon Dots (SPION-CDs), for fluorescence and magnetic resonance imaging is introduced. This nanoparticle possesses the magnetic properties of super-paramagnetic iron oxide (SPION) core as well as the fluorescence characteristics of carbon dots (CDs) coated in mesoporous structure. The SPION-CDs were synthesized using a high temperature facile single-pot hydrothermal method. The products were characterized by transmission electron microscopy (TEM), dynamic light scattering (DLS), X-ray diffraction (XRD), UV/vis absorption, vibrating sample magnetometer (VSM). The cytotoxic effect of SPION-CDs on OVCAR-3 cells was also evaluated. The synthesized nanoparticle possesses optimal size, low toxicity and excellent magnetic properties, including super-paramagnetic behavior ($M_s = 42 \text{ emu g}^{-1}$). Moreover,

* Masoud A, Mehrgardi, *e-mail*: m.mehrgardi@chem.ui.ac.ir or m.mehrgardi@gmail.com

* Parvaneh, Shokrani, *e-mail*: shokrani@med.mui.ac.ir

in the viewpoint of optical properties, the quantum yield of $\sim 2.4\%$ was obtained and the nanoparticle shows good fluorescence stability for cell-labeling studies. This multifunctional nanoparticle with appropriate characterization is a promising candidate for multimodal fluorescence/magnetic resonance imaging platform.

Keywords: Multifunctional nanoparticle; Super Paramagnetic Iron Oxide Nanoparticle; Carbon Dots

Introduction

Magnetic resonance imaging (MRI) and fluorescence imaging (FI) are two common modalities used in clinical diagnostic practice. MRI is a non-invasive imaging modality with high spatial and temporal resolution, but its sensitivity is rather low.¹ In contrast, FI is the most versatile modality used in real-time imaging, localization of tumors and metastases and monitoring of various biological progression or regression with high sensitivity at the molecular level. However, because of limited penetration and increased absorption of light by the surrounding tissue, it has relatively poor spatial resolution compared to anatomical imaging.²

Recently, biomedical imaging with multifunctional nanoparticles such as multimodal MRI/FI nanoprobe has attracted a great deal of attention due to increased accuracy in diagnosis by providing high-resolution 3D and high-sensitive functional images.³ Because of advanced imaging properties of nanomaterial-based imaging agents, a number of representative nanomaterials with a single imaging modality are used in research and clinical practice. Quantum dots (QDs), generally semiconductor nanocrystals, have attracted increasing interest in biomedical researching fields in recent years due to good fluorescent property.⁴ Carbon-based nanoparticles, especially carbon dots (CDs) with similar optical properties with quantum dots have recently received much attention in the

field of fluorescence imaging.⁵ CDs disperse well in water and usually show optical absorption band around 260-320 nm. Carbon dots have also been found to be nontoxic and biocompatible which are suitable for biological systems. Other advantages include rapid cellular uptake, high fluorescence brightness, excellent water solubility and high photo-stability.^{4,6} Iron-oxide nanoparticles (Fe_3O_4 or $\gamma\text{-Fe}_2\text{O}_3$) are the most prominent negative contrast agents that are widely used in MRI for their biocompatible nature because of cell iron metabolism pathways and strong effects on T_2 and T_2^* relaxation.⁷ High signal amplification ability per unit of metal, chemical linkage ability with functional groups/ligands and detectable by light and electron microscopy are other popularity properties of super paramagnetic iron oxide particles.⁷⁻⁸

Multimodal fluorescence/magnetic nanoparticles have been synthesized to overcome the limitations of single imaging FI and MRI modalities, i.e. to provide both high-resolution information and high-sensitive functional images. The goal was to take advantage of carbon dot and super paramagnetic iron oxide nanoparticle properties in FI and MRI, simultaneously. This manuscript presents the synthesis and characterization of SPION-CDs for MRI/FI imaging.

Results and Discussion

In the present study, multifunctional magnetic and fluorescent nanoparticles were prepared based on a high temperature facile single-pot hydrothermal method. According to the synthesis method, CDs were assembled on the surface of the mesoporous structure of SPIONs. The morphology and structure characterization of synthesized NP is shown in Figure 1. The average hydrodynamic diameter of SPION-CDs in water

measured by the dynamic light scattering and was around 43 nm (Figure 1a). The transmission electron microscopy image shows SPION-CDs are spherical with size of less than 50 nm (Figure 1b). The cell uptake of NPs has great influence on their biomedical functions, such as drug delivery. Size of nanoparticles can influence their cellular uptake, as studied by Chithrani et al.⁹ They synthesized nanoparticles of 1-100 nm diameter range and reported 50 nm as the optimal size for maximum cell uptake. Therefore, it is concluded that SPION-CDs can potentially be used for drug delivery, due to the porous structure and optimal particle size.

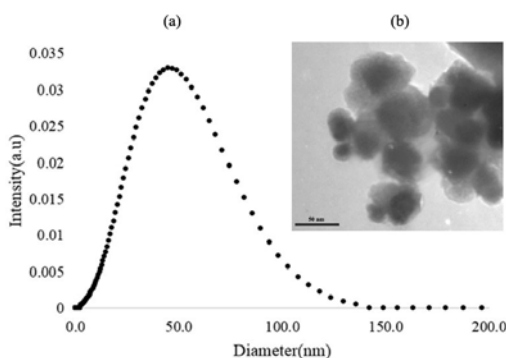
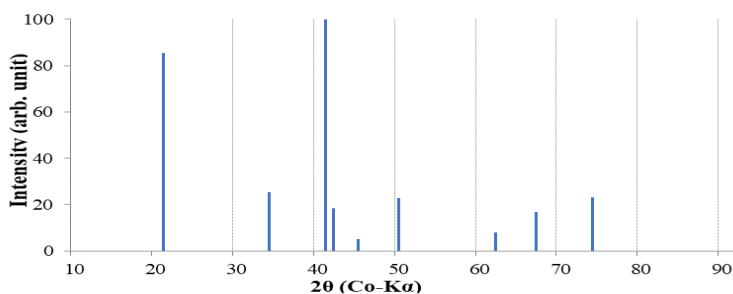


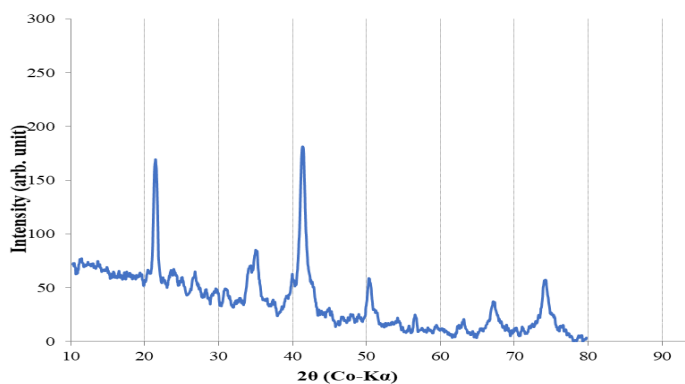
Figure 1. (a) Particle diameter distribution of SPION-CDs; (b) TEM image of SPION-CDs.

To clarify the phase and structure of our nanoparticle, XRD experiment was carried out. X-ray diffraction (XRD) measurements were carried out with Co-K α radiation ($\lambda = 0.1789$ nm) generated at 30 kV and 30 mA. The XRD patterns of the synthesized nanoparticles are shown in Figure 2. The peak positions are in-line with the spinel structure. Therefore, the synthesized nanoparticles are Fe₃O₄ and/or γ -Fe₂O₃ phases. Although the patterns of Fe₃O₄ and γ -Fe₂O₃ phases are similar, the absence of some peaks corresponding to γ -Fe₂O₃ phase, such as (110), (210) and (211) peaks, is a good evidence that approves the synthesized nanoparticles are in Fe₃O₄

phase. In these diffraction patterns, no trace of the reactants and by-products, i.e. FeCl_3 , NaOH , NaCl and so on, can be seen. As shown in Figure 2, eight relatively discernible diffraction peaks of Fe_3O_4 at $2\theta = 21.4^\circ$, 35.0° , 41.4° , 42.9° , 50.2° , 62.4° , 67.1° and 74.1° are indexed to (111), (220), (311), (222), (400), (422), (511) and (440) planes, respectively. The peaks at 2θ of 41° - 60° should belong to Iron carbides such as Fe_2C (PDF-17-0897) and Fe_5C_2 (PDF-36-1248), which overlap some Fe_3O_4 peaks.¹⁰⁻¹¹ Moreover, the crystallite size was calculated ~ 22 nm using the Scherrer's equation based on the width of the spinel (311) peak ($2\theta=41.4^\circ$) in Figure 2. It's worthy to mention that the hydrodynamic diameter of SPION-CDs is around two times larger than crystallite size, indicating effective hydration of nanoparticles.



a



b

Figure 2. XRD patterns of: a) JCPDS reference patterns of the Fe_3O_4 (No. 19-0629); b) super paramagnetic iron oxide nanoparticle-carbon dots (SPION-CDs).

To investigate the multimodal FI/MRI application potential of this nanoparticle, the optical characteristics of SPION-CDs were studied. Figure 3 shows the photoluminescent (PL) emission and excitation spectra of the SPION-CDs. These nanoparticles demonstrated PL properties, including excitation spectra with a maximum peak at 350 nm and emission spectra around 450 nm. Excellent PL properties, including broad excitation spectra and symmetric emission spectra, are ideal for multicolor probes and enable us to select the excitation wavelength from a broad excitation spectrum. Therefore, it is straightforward to separate excitation and emission spectra of CDs in comparison with organic dyes which have narrow absorption and asymmetric emission spectra.¹²

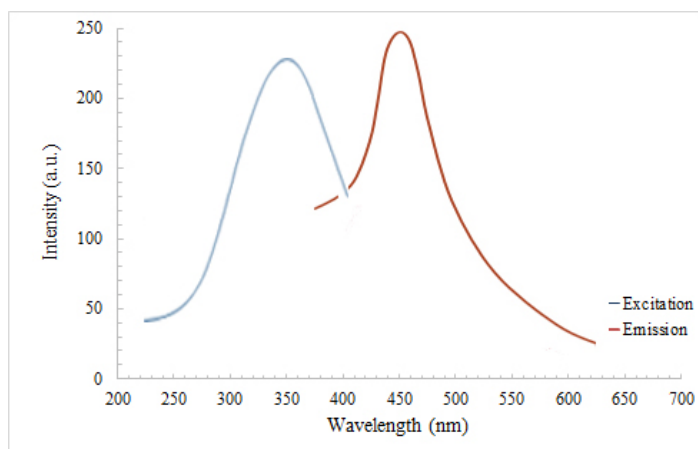


Figure 3. Optical properties: excitation and emission spectrum of SPION-CDs. The maximum emission peak was observed at 450 nm for the excitation wavelength of 350 nm.

Quantum yield (QY), defined as the ratio of the number of emitted photons to the number of absorbed photons per time unit, is a significant parameter to characterize PL.¹³ The QY of the SPION-CDs was estimated to be 2.4%. A value of QY, over the range of 1 to 5%, is sufficient for cell-labeling studies.¹⁴ Moreover, different synthetic routes, N-doping, surface modifications and various purification procedures can lead to the higher

values of QY for CDs.^{12b} One of the reasons for low quantum yield is the electronic coupling and energy transfer between magnetic cores and CDs; resulting in a fluorescent quenching effect.

The fluorescence stability of SPION-CDs was assessed using a luminescence spectrometer. Results showed 5% decrease in photoluminescence intensity after 24 hours at room temperature, indicating insignificant aggregation and/or variation in fluorescence quantum yield (Figure 4a). As observed in Figure 4b and c, SPION-CDs can disperse in water easily, and an aqueous suspension exhibits a shade of yellowish brown in daylight and bright-green fluorescence under UV light. The response of SPION-CDs to an external handheld magnet is satisfactory, i.e. after collecting SPION-CDs by a magnet, the supernatant does not exhibit any fluorescence, indicating the optical/magnetic characteristics of SPION-CDs.

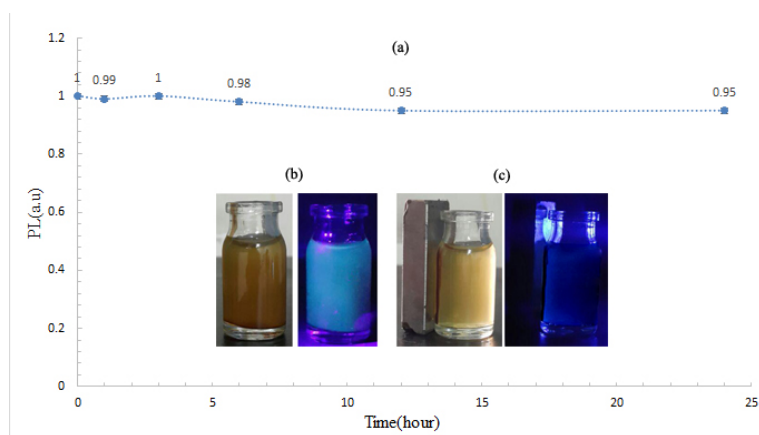


Figure 4. (a) The fluorescence stability of SPION-CDs during 24 h. The inset photographs show the SPION-CDs solution under visible (left row) and UV light (right row) without (b) and with (c) an external handheld magnet.

The magnetic properties of the SPION-CDs were investigated by studying the field-dependent magnetization curves at room temperature. Figure 5 illustrates the magnetic hysteresis loops of SPION-CDs. The

saturation magnetization of SPION-CDs was ~ 42 emu/g, slightly lower than 44.5 emu/g and 51.2 emu/g reported for $\text{Fe}_3\text{O}_4/\text{SiO}_2$ and Fe_3O_4 nanoparticles, respectively.¹⁵ The difference may be attributed to mesoporous carbon shell and CDs surrounding the magnetic cores. The difference between our saturation magnetization value (42 emu/g) and the 32.5 emu/g value reported by Wang et al. is related to the slight differences in the synthesis procedure.¹⁶ Results showed no remanence and coercivity, approving the super-paramagnetic property of the nanoparticle.

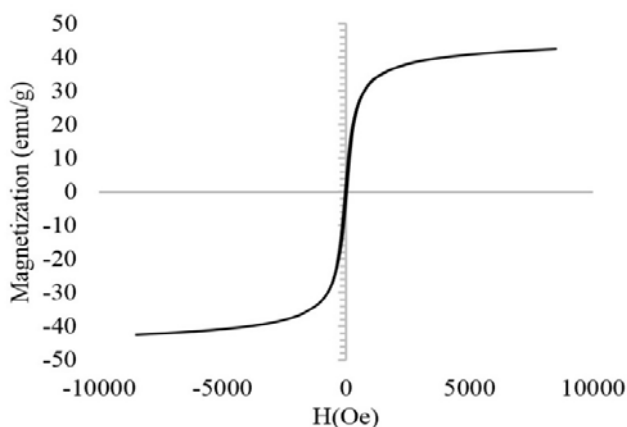


Figure 5. Magnetic properties: the magnetic hysteresis loop of SPION-CDs measured at room temperature.

The low toxicity and biocompatibility are important for fluorescent/magnetic nanoparticles used as contrast agents, drug delivery and in biological medicine field. Figure 6 shows the cell viability after incubation with 0–1000 mg/mL of SPION-CDs nanoparticles. The viability of the OVCAR-3 cells still remained above 80% after 24 and 48 h incubation with SPION-CDs even at the concentration of 40 $\mu\text{g}/\text{mL}$. So according to our MTT results, SPION-CDs have low toxicity and are good candidates in the biological applications.

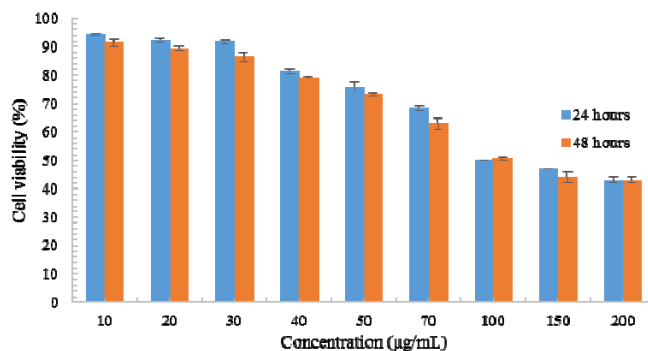


Figure 6. Cell viability mean percent values of OVCAR-3 affected by increasing concentrations during 24 and 48 h incubation (error bars indicate \pm SD).

Experimental

Materials

The chemical reagents, such as ferrocene ($\text{Fe}-(\text{C}_5\text{H}_5)_2$, $\geq 98\%$), hydrogen peroxide (H_2O_2 , 30%) and acetone ($\text{C}_3\text{H}_6\text{O}$, 99.5%) were purchased from Sigma. The OVCAR-3 cancer cell lines were purchased from the Cell Center of Pasteur Institute of Iran.

Synthesis of SPION-CDs

Briefly, 0.10 g ferrocene, as the precursor, was dissolved in 30 mL acetone. Subsequently, 5 mL of hydrogen peroxide (H_2O_2 -30%) was slowly added to this solution while stirring for 30 min. The prepared solution was then heated in an autoclave at 200 °C for 48 h. After cooling to room temperature, the product was collected using a magnet and was washed three times with acetone. The obtained product was finally dried under vacuum overnight.

Characterization of the nanoparticles

The hydrodynamic diameter was measured at 25 °C using Dynamic Light Scattering (DLS) with the detector angle of 90° (VASCO, France)

after filtration of the suspensions with a 0.22 μm filtration membrane to remove aggregated particles. The size and morphology of nanoparticles were examined using a transmission electron microscope (TEM) (Philips CM200, Netherlands). Magnetic properties and magnetic hysteresis loop of nanoparticles were measured using a vibrating sample magnetometer (VSM) (Daghigh Meghnatis Kashan Co., Iran) at room temperature. Photoluminescence (PL) spectra were measured by a fluorescence spectrophotometer (Shimadzu RF5301, Japan) in the 200-700 nm wavelength range. UV-visible absorption spectra were acquired using TU-1901 UV-Vis spectrophotometer (Shimadzu, Japan). X-ray diffraction measurements were conducted by Co-K α to investigate the sample structure (Bruker, Germany).

In vitro cytotoxicity study

To evaluate the cytotoxicity of SPION-CDs, the MTT assay was performed. OVCAR-3 cells were cultured in Roswell Park Memorial Institute (RPMI) supplemented with 10% fetal bovine serum (FBS) and 1% (v/v) penicillin-streptomycin at 37 °C in a 5% CO₂ and were seeded at a density of 20×10^4 cells/mL in 96 well plates. After 24 h, SPION-CDs nanoparticles were added to the cells with various concentrations over a range of 0–1000 mg/mL for 24 and 48 h. Then, 20 mL of MTT solution was added to each well and incubated for 2 h. After removing the supernatant, 150 μL of DMSO was added to each well and the absorbance was measured at 570 nm wavelength using a microplate reader. The cell viability (%) was calculated according to the following equation, where OD sample and OD control are the samples and control optical density.

$$\text{Cell viability (\%)} = \text{OD sample} / \text{OD control} * 100.$$

Conclusions

In summary, a strategy to synthesize a fluorescent/magnetic nanoparticle with appropriate magnetic and optical properties was introduced. The SPION-CDs exhibit optimal size, low toxicity and good magnetic/optical property. In the viewpoint of optical and magnetic properties, appropriate quantum yield, fluorescence stability and super-paramagnetic property are comparable to other contrast agents. SPION-CDs represent a fluorescence/magnetic resonance imaging agents that may serve as a multifunctional clinical tool.

Acknowledgments

The authors would like to acknowledge the financial support of this research by Isfahan University of Medical Sciences (no. 396461) and University of Isfahan Research Council.

References

1. Iyer, V.R.; Lee, S.I. MRI, CT, and PET/CT for ovarian cancer detection and adnexal lesion characterization. *AJR Am. J. Roentgenol.* **2010**, *194*(2), 311-321.
2. Ntziachristos, V. Fluorescence molecular imaging. *Annu. Rev. Biomed. Eng.* **2006**, *8*, 1-33.
3. Chen, H.; Wang, Y.; Wang, T.; Shi, D.; Sun, Z.; Xia, C.; Wang, B. Application prospective of nanoprobe with MRI and FI dual-modality imaging on breast cancer stem cells in tumor. *J. Nanobiotechnology* **2016**, *14*(1), 52.
4. Luo, P.G.; Sahu, S.; Yang, S.-T.; Sonkar, S.K.; Wang, J.; Wang, H.; LeCroy, G.E.; Cao, L.; Sun, Y.-P. Carbon “quantum” dots for optical bioimaging. *J. Mater. Chem. B* **2013**, *1*(16), 2116-2127.
5. Sun, Y.-P.; Zhou, B.; Lin, Y.; Wang, W.; Fernando, K.S.; Pathak, P.; Mezziani, M.J.; Harruff, B.A.; Wang, X.; Wang, H., Quantum-sized carbon dots for bright and colorful photoluminescence. *J. Am. Chem. Soc.* **2006**, *128*(24), 7756-7757.
6. Lim, S.Y.; Shen, W.; Gao, Z. Carbon quantum dots and their applications. *Chem. Soc. Rev.* **2015**, *44*(1), 362-381.

7. Na, H.B.; Song, I.C.; Hyeon, T. Inorganic nanoparticles for MRI contrast agents. *Adv. Mater.* **2009**, *21*(21), 2133-2148.
8. Wei, H.; Bruns, O.T.; Kaul, M.G.; Hansen, E.C.; Barch, M.; Wiśniowska, A.; Chen, O.; Chen, Y.; Li, N.; Okada, S. Exceedingly small iron oxide nanoparticles as positive MRI contrast agents. *Proc. Natl. Acad. Sci. U.S.A.* **2017**, *114*(9), 2325-2330.
9. Chithrani, B.D.; Ghazani, A.A.; Chan, W.C. Determining the size and shape dependence of gold nanoparticle uptake into mammalian cells. *Nano Lett.* **2006**, *6*(4), 662-668.
10. Nasser, A.-H.; Guo, L.; ELnaggar, H.; Wang, Y.; Guo, X.; AbdelMoneim, A.; Tsubaki, N. Mn-Fe nanoparticles on a reduced graphene oxide catalyst for enhanced olefin production from syngas in a slurry reactor. *RSC Adv.* **2018**, *8*(27), 14854-14863.
11. Todaka, Y.; Nakamura, M.; Hattori, S.; Tsuchiya, K.; Umemoto, M. Synthesis of ferrite nanoparticles by mechanochemical processing using a ball mill. *Mater. Trans.* **2003**, *44*(2), 277-284.
12. (a) Resch-Genger, U.; Grabolle, M.; Cavaliere-Jaricot, S.; Nitschke, R.; Nann, T. Quantum dots versus organic dyes as fluorescent labels. *Nat. Methods* **2008**, *5*(9), 763; (b) Miao, P.; Han, K.; Tang, Y.; Wang, B.; Lin, T.; Cheng, W., Recent advances in carbon nanodots: synthesis, properties and biomedical applications. *Nanoscale* **2015**, *7*(5), 1586-1595.
13. Laverdant, J.; Marcillac, W.D.; Barthou, C.; Chinh, V.D.; Schwob, C.; Coolen, L.; Benalloul, P.; Nga, P.T.; Maître, A. Experimental determination of the fluorescence quantum yield of semiconductor nanocrystals. *Materials* **2011**, *4*(7), 1182-1193.
14. Erogbogbo, F.; Yong, K.-T.; Roy, I.; Xu, G.; Prasad, P.N.; Swihart, M. T. Biocompatible luminescent silicon quantum dots for imaging of cancer cells. *ACS Nano* **2008**, *2*(5), 873-878.
15. Du, G.; Liu, Z.; Xia, X.; Chu, Q.; Zhang, S. Characterization and application of Fe₃O₄/SiO₂ nanocomposites. *J. Sol-Gel Sci. Technol.* **2006**, *39*(3), 285-291.
16. Wang, H.; Shen, J.; Li, Y.; Wei, Z.; Cao, G.; Gai, Z.; Hong, K.; Banerjee, P.; Zhou, S. Magnetic iron oxide-fluorescent carbon dots integrated nanoparticles for dual-modal imaging, near-infrared light-responsive drug carrier and photothermal therapy. *Biomater. Sci.* **2014**, *2*(6), 915-923.